MPS-FEM Coupled Method for Interaction between Sloshing Flow and Elastic Structure in Rolling Tanks

Youlin Zhang, Zhenyuan Tang, Decheng Wan*

State Key Laboratory of Ocean Engineering, School of Naval Architecture, Ocean and Civil Engineering, Shanghai Jiao Tong University, Collaborative Innovation Center for Advanced Ship and Deep-Sea Exploration, Shanghai 200240, China

*Corresponding author: dcwan@sjtu.edu.cn

Abstract

A coupling improved Moving Particle Semi-Implicit (MPS) method and the finite element method (FEM) is developed and applied to the problem of interaction between elastic structures and the violent sloshing flow in rolling tanks. The MPS method and the FEM, used to calculate the fluid field and structural deformation respectively, are introduced firstly. Then, the coupling strategy is also presented. To validate accuracy of the proposed algorithm for deformation of an elastic structure, two benchmarks are investigated and present results show good agreement with published data. Finally, cases about the sloshing with thin elastic baffles mounted in the partially filled rolling tanks are numerically studied. Both profiles of free surface and deflections of the baffles are in good agreement with experimental data.

Keywords: Particle method; Moving Particle Semi-Implicit (MPS); finite element method (FEM); Fluid structure interaction (FSI); Sloshing; Roll motion

Introduction

Fluid structure interaction (FSI) problems are commonly existent in ship and ocean engineering, such as sloshing in liquid containers while vessels sailing on very rough sea. Due to the impact loads induced by the periodic motion of inner liquid, the bulkheads or baffles mounted inside the tank may be deformed or even damaged. Hence, the investigation about interaction between the violent sloshing flow and the structures is useful for the assessment of safety of liquid containers.

For a typical FSI problem, the whole computational domain contains the fluid domain and the structural domain. Accurate prediction of the fluid computational domain is one of the key aspects for FSI problems. Generally speaking, numerical algorithms for the fluid domain simulation can be divided into two categories, the grid based methods and the meshless methods [1]. The grid based methods, such as the finite difference method (FDM), finite volume method (FVM), and finite element method (FEM), are much popular in the simulation of fluid domain. However, the main challenges of these approaches include inefficient process of grids generation for complex shape of structure, complex technology of dynamic mesh for moving boundary or structural deformation, simulation of free surface with large deformation or breaking, etc [2]. On the contrary, the meshless methods are in good performance to settle these challenges. One representative Lagrangian particle method for free surface flows is the MPS method which is originally proposed by Koshizuka and Oka [3] for incompressible flow. Since lots of improvements were proposed to suppress the numerical unphysical pressure oscillation [4]-[10], the MPS method can be employed to deal with kinds of hydrodynamic problems. Such as dam-breaking flow [11], water-entry flow [12]-[14], wave-float interaction

problem [2][15][16], sloshing in liquid tank [1][17], impinging jet flow [18], etc. In this paper, the MPS method is employed for the computation of fluid domain in FSI problem.

For the calculation of structural domain, deformation of structure is commonly computed based on the modal superposition analysis or the FEM method. Though the modal superposition analysis is easy to formulate and programming [19], it's incapable of solving large and nonlinear deformation of structure. Relatively, FEM method is widely employed to deal with structural deformation [20]-[25] and adopted in many commercial software, such as ABAQUES, ANSYS, MSC.NASTRAN, etc. In present research, both linear and nonlinear deformations of baffles inside in the rolling tank will be investigated based on the FEM method.

In the FSI simulations, the coupling strategies between fluid solver and structural solver can be classified into two groups: the strong coupling approach and the weak coupling approach. In the strong coupling approach, a single system equation involving all variables related to both the fluid and structure dynamics is solved simultaneously [26]. However, the equation is much difficulty to form without any modification for complex engineering problems [27] and much expensive to be solved [28]. On the contrary, the fluid and structure fields are self-governed by different equations and solved separately in the weak coupling approach. Interfacial information communicates explicitly between the fluid and structure solution. This approach allows the use of separated fluid and structure codes or established software for each computational domain [23], and it is suitable to deal with engineering problems with large deformation. Hence, the weak coupling approach is utilized in the present paper.

The main object of this study is to develop a MPS-FEM coupled method which can be applied in nonlinear FSI problems, such as the interaction between sloshing flow in a rolling tank and elastic structure. The paper is organized as follows. Firstly, the MPS method is briefly reviewed. Next, the FEM method and the coupling strategy are described. Accuracy of the structure solver is validated by two benchmarks of dynamic oscillating beams. Then, the MPS-FEM coupled solver is applied to the problem of liquid sloshing in a tank interacting with baffles which will deform nonlinearly. Accuracy of the proposed method are verified by comparison against experimental data and simulation data from Idelsohn et al [21].

Numerical methods

In present study, the fluid domain is calculated by our in-house particle solver MLParticle-SJTU based on improved MPS method. Details about the improvements and validation of the solver can be find in the published literatures [1][11][17][18]. In this section, a brief review about the structure solver and the MPS-FEM coupling strategy is described as fellow.

Structure solver based on FEM
Based on Hamilton's principle, deformation of structure should satisfy

$$\delta H = 0, \quad H = \int_{t_1}^{t_2} [T - \Pi_s + \Pi_p] \mathrm{d}t \tag{1}$$

where T is the kinetic energy, Π_s is the strain energy, Π_p is the potential energy of external force and damping force.

According to previous literatures [29], the structural dynamic equations, which governing the motion of structural elements, can be derived from Eq. (1) and expressed as

$$\mathbf{M}\ddot{y} + \mathbf{C}\dot{y} + \mathbf{K}\,y = F(t) \tag{2}$$

$$\mathbf{C} = \alpha_1\mathbf{M} + \alpha_2\mathbf{K} \tag{3}$$

where $\mathbf{M}$, $\mathbf{C}$, $\mathbf{K}$ are the mass matrix, the Rayleigh damping matrix, the stiffness matrix of the structure, respectively. F is the external force vector acting on structure, and varies with computational time. y is the displacement vector of structure. α_1 and α_2 are coefficients which are related with natural frequencies and damping ratios of structure.

To solve the structural dynamic equation, another two group functions should be supplemented to set up a closed-form equation system. Here, Taylor's expansions of velocity and displacement developed by Newmark [30] are employed:

$$\dot{y}_{t+\Delta t} = \dot{y}_t + (1-\gamma)\ddot{y}_t\Delta t + \gamma\ddot{y}_{t+\Delta t}\Delta t \quad , \quad 0 < \gamma < 1 \tag{4}$$

$$y_{t+\Delta t} = y_t + \dot{y}_t\Delta t + \frac{1-2\beta}{2}\ddot{y}_t\Delta t^2 + \beta\ddot{y}_{t+\Delta t}\Delta t^2 \quad , \quad 0 < \beta < 1 \tag{5}$$

where β and γ are important parameters of the Newmark method, and selected as β=0.25, γ=0.5 for all simulations in present paper. From Eq. (2-5), the displacement at $t=t+\Delta t$ can be solved by the following formula [31]:

$$\bar{\mathbf{K}}\,y_{t+\Delta t} = \bar{F}_{t+\Delta t} \tag{6-a}$$

$$\bar{\mathbf{K}} = \mathbf{K} + a_0\mathbf{M} + a_1\mathbf{C} \tag{6-b}$$

$$\bar{F}_{t+\Delta t} = F_t + \mathbf{M}(a_0 y_t + a_2\dot{y}_t + a_3\ddot{y}_t) + \mathbf{C}(a_1 y_t + a_4\dot{y}_t + a_5\ddot{y}_t) \tag{6-c}$$

$$a_0 = \frac{1}{\beta\Delta t^2}, \; a_1 = \frac{\gamma}{\beta\Delta t}, \; a_2 = \frac{1}{\beta\Delta t}, \; a_3 = \frac{1}{2\beta} - 1, a_4 = \frac{\gamma}{\beta} - 1,$$

$$a_5 = \frac{\Delta t}{2}(\frac{\gamma}{\beta} - 2), a_6 = \Delta t(1-\gamma), \; a_7 = \gamma\Delta t \tag{6-d}$$

where $\bar{\mathbf{K}}$ and $\bar{F}$ are so-called effective stiffness matrix and effective force vector, respectively. Finally, the accelerations and velocities corresponding to the next time step are updated as follows.

$$\ddot{y}_{t+\Delta t} = a_0(y_{t+\Delta t} - y_t) - a_2\dot{y}_t - a_3\ddot{y}_t \tag{7}$$

$$\dot{y}_{t+\Delta t} = \dot{y}_t + a_6\ddot{y}_t + a_7\ddot{y}_{t+\Delta t} \tag{8}$$

To validate the accuracy of present structural solver, two test cases are carried out. In the first case, response of the undamped cantilever beam under a ramp-infinite duration load is studied. The sketches of beam geometry and load history are shown as Fig. 1 and Fig. 2. The Young's modulus, density, moment of inertia, and cross area of the structure are 30×10^6 psi, 4.567×10^{-3} lb s^2/in^4, 100 in^4 and 21.9 in^2, respectively. Time history about the displacement at the tip of the undamped cantilever is shown as Fig. 3. According to the comparison between present result and Behdinan's data [34], good agreement can be achieved.
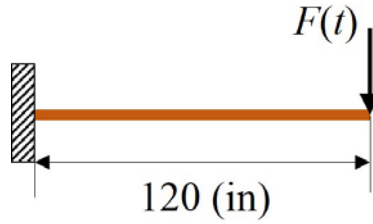
Figure 1.   Beam geometry
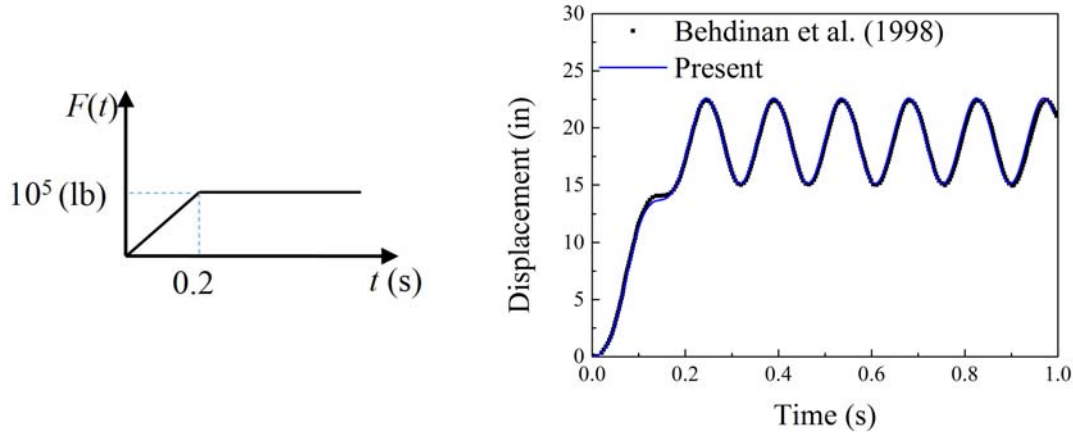
Figure 2.Load history of test 1

Figure 3.   Time response of the tip (test 1)

In the FEM method, response of structure is obviously related to viscous damp coefficients. Hence, the second test case about the damped cantilever beam under a ramp-ramp duration load is studied. The sketches of beam geometry is same as that in test case 1 and shown as Fig. 1. The load history is shown as Fig. 4. The Young's modulus, density, moment of inertia, and cross area of the structure are all same as the first test case. However, the effect of damp is considered and the Rayleigh's coefficients are set $\alpha_1 = 0.0$, $\alpha_2 = 0.003$. Time history about the displacement at the tip of the damped cantilever is shown as Fig. 5. Present result and Behdinan's data are in good agreement. So, present structural solver is suitable to solve deformation of structure.
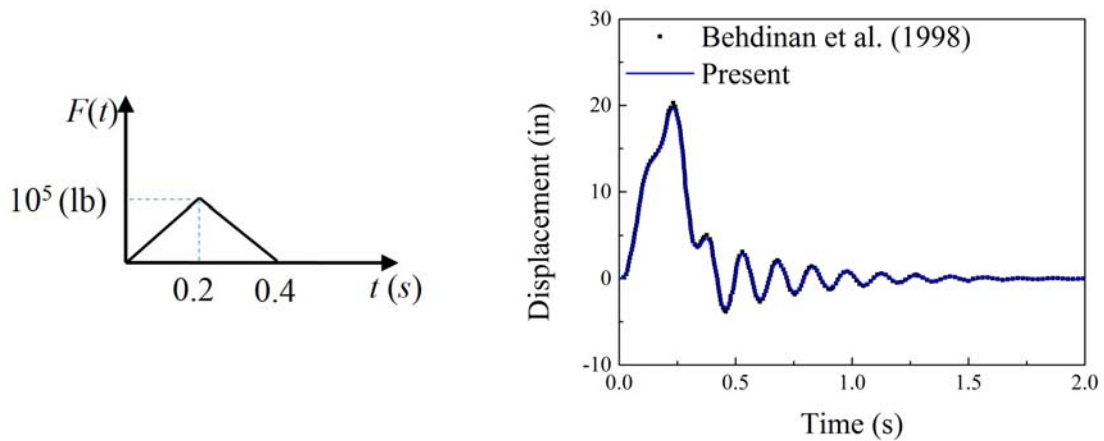
Figure 4.   Load history of test 2

Figure 5.   Time response of the tip (test 2)

MPS-FEM coupling strategy

In present study, the weak coupling between MPS and the FEM method is implemented. Flowchart of solution procedure is shown as Fig. 6. Sizes of time step for structure analysis and fluid analysis are Δt_s and Δt_f, respectively. Here, Δt_s is k multiples of Δt_f, where k is an integer. The procedure of interaction can be summarized as below.

(1) The fluid field would be calculate k times based on MPS method. Pressure of fluid wall boundary particle is calculated as follows:

$$\bar{p}_{n+1} = \frac{1}{k} \sum_{i=1}^{k} p_{n+i} \tag{9}$$

where p_{n+i} is pressure of the fluid particle on wall boundary at the instant $t + i\Delta t_f$, $\bar{p}_{n+1}$ is averaged pressures of fluid particle within Δt_s.

(2) Determine the values of structural nodal position y_t, velocity $\dot{y}_t$ and acceleration $\ddot{y}_t$ based on the results of previous time step.

(3) Calculate external force vector $F_{t+\Delta t_s}$ of structural boundary particles based on pressure of fluid wall boundary particles $\bar{p}_{n+1}$.

(4) Calculate the new values of structural nodal displacements and velocities based on the Newmark method described in the previous section.

(5) Update velocity and position of both structural boundary particles and fluid particles.
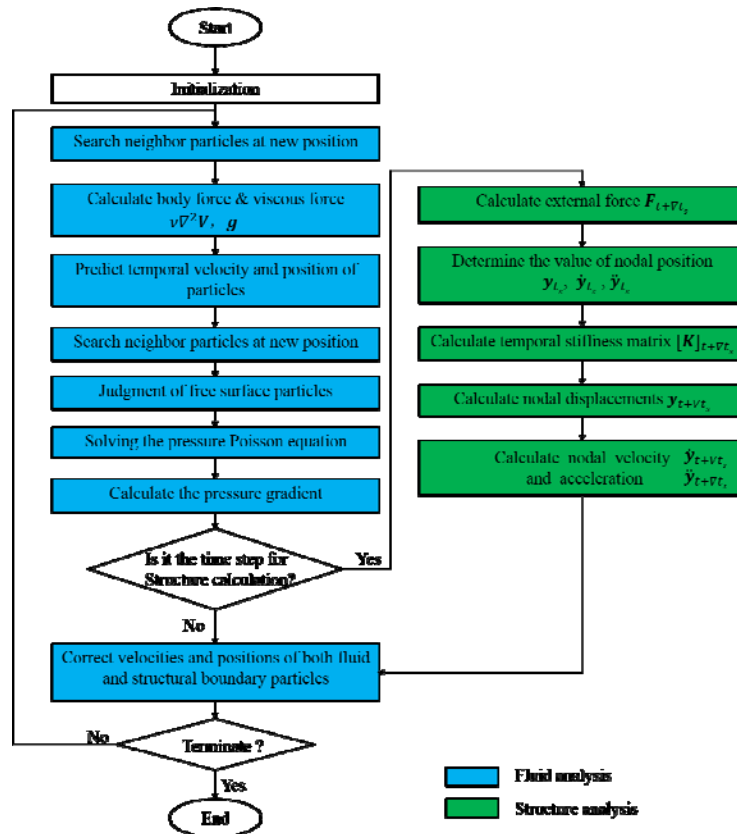
Figure 6.   Flowchart of MPS-FEM coupling procedure

Numerical Simulations

In present study, the MPS-FEM coupled method is used to simulate the interaction between sloshing flow and elastic structure in a 2D rolling tank. The experimental data published by Idelsohn et al. [21] and the numerical result published by Paik [32][33] are used for comparison study and validation of the capability of present numerical method.

Numerical setup

According to the experiments carried out by Idelsohn [21], three cases are numerically investigated in this paper. Elastic baffles are mounted at the bottom or top of the two-dimensional tank and related sketches about the geometry setup are shown as Fig. 7. The tank, with a length of 609 mm and a height of 344.5mm, is free to roll around the point O which is the center of bottom of the container. The tank is forced to roll harmoniously with the governing equation of motion defined as

$$\theta(t) = \theta_0 \sin(\omega t) \tag{10}$$

where $\theta(t)$ is the rotation angle of the tank, θ_0 is the excitation amplitude, ω is the angular frequency.
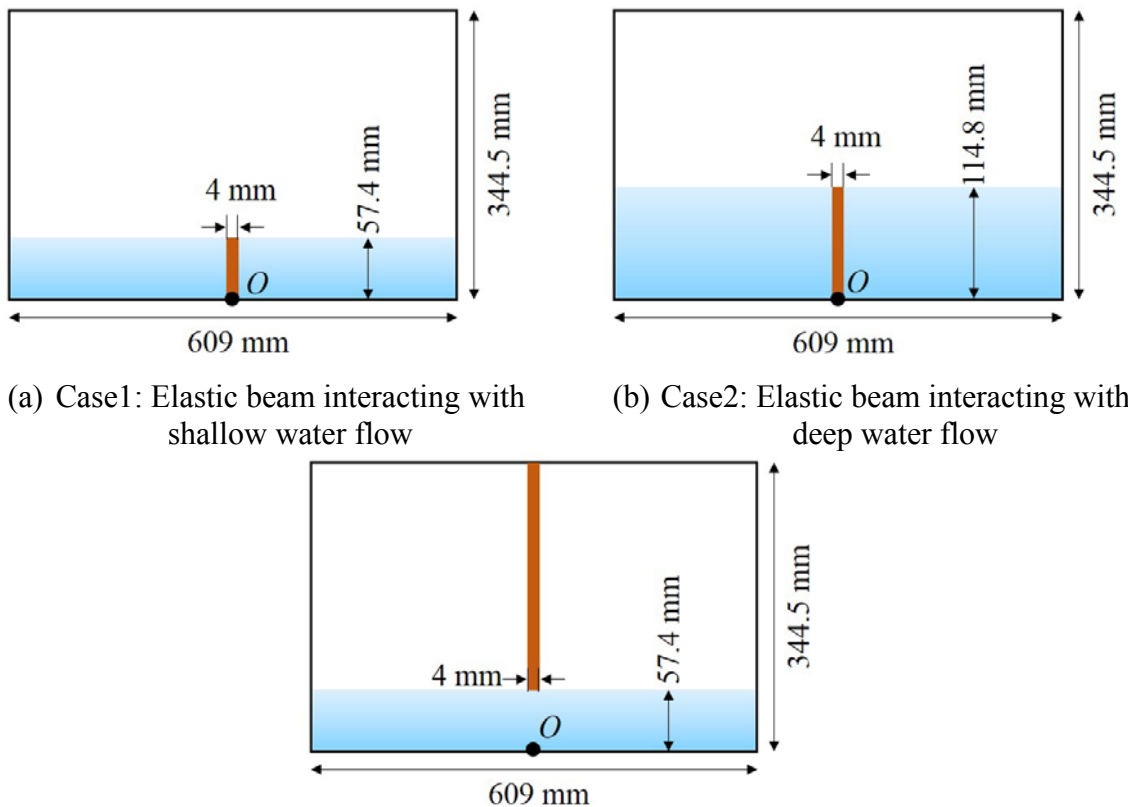
(a) Case1: Elastic beam interacting with shallow water flow

(b) Case2: Elastic beam interacting with deep water flow

(c) Case3: Hanging elastic beam interacting with shallow water flow

Figure 7.   Sketches of the rolling tank with elastic beams

Table 1.   Fluid parameters of numerical cases

Parameters	Case 1	Case 2	Case 3
Fluid density (kg/m^3)	917	917	998
Kinematic viscosity (m^2/s)	5×10^{-5}	5×10^{-5}	1×10^{-6}
Gravitational acceleration (s/m^2)	9.81	9.81	9.81
Fluid depth (mm)	57.4	114.8	57.4
Rolling frequency (Hz)	0.61	0.83	0.61
Rolling amplitude (degree)	4	4	2
Particle spacing (mm)	2	2	2
Time step size (s)	2×10^{-4}	2×10^{-4}	2×10^{-4}

Table 2.   Structure parameters of numerical cases

Parameters	Case 1	Case 2	Case 3
Structure density (kg/m^3)	1100	1100	1900
Young's modulus (Pa)	6×10^6	6×10^6	4×10^6
Length (mm)	57.4	114.8	287.1
Clamped position	Bottom	Bottom	Top
Number of elements	29	58	145
Damping coefficients α1	0	0	0
Damping coefficients α2	0.05	0.025	0.025
Time step size (s)	2×10^{-3}	2×10^{-3}	2×10^{-3}

Elastic beam interacting with shallow water flow

In present case, the tank, rolling with the amplitude of 4 degrees and frequency of 0.61 Hz, is partially filled with fluid of 57.4 mm depth. Density and Kinematic viscosity are 917 kg/m^3 and 5×10^{-5} m^2/s, respectively. A short baffle is mounted at the rolling center point *O*. Length and width of the baffle are 57.4 mm and 4 mm. Density and the Young's modulus of the baffle are 1100 kg/m^3 and 6×10^6 Pa, respectively. The models of both fluid and structure are dispersed by particles with spacing of 2 mm. The baffle is simplified as a beam and dispersed by 29 elements. The coefficients of $\alpha_1 = 0.0$ and $\alpha_2 = 0.05$ are used to compose the structural Rayleigh damping matrix **C** which is an important part of the dynamic equations. The size of time steps is 0.0002 s for the calculation of fluid domain while that is 0.002 s for the structural domain.

Snapshots about deformation of baffle and elevation of free surface are shown in Fig. 8. Numerical data is compared with experiment at four instants, t=0.95, 1.35, 1.62, and 1.88 s. Profiles of the deformed baffle and free surface are coincident with that of experiment. However, a bubble cavity, which doesn't exist in the experiment, forms near the top of baffle while the fluid flows over the structure in present simulation. As mentioned in Paik et al. [33], the possible reason about the babble cavity is the three dimensional nature that the channel is open and air is able to escape for the real flow. Generally, the agreement between the numerical results and the experimental ones are acceptable.

Time histories of the horizontal displacement at the top tip of baffle are shown as Fig. 9. Present numerical result based on MPS-FEM method is compared with experimental data of Idelsohn [21] and simulation results from both Idelsohn and Paik [33]. The trend of numerical curve evolves harmonically and with a period similar to experiment. Though the amplitude of

present numerical curve is larger than experiment, it's similar to the simulation results published by Paik et al. [33].
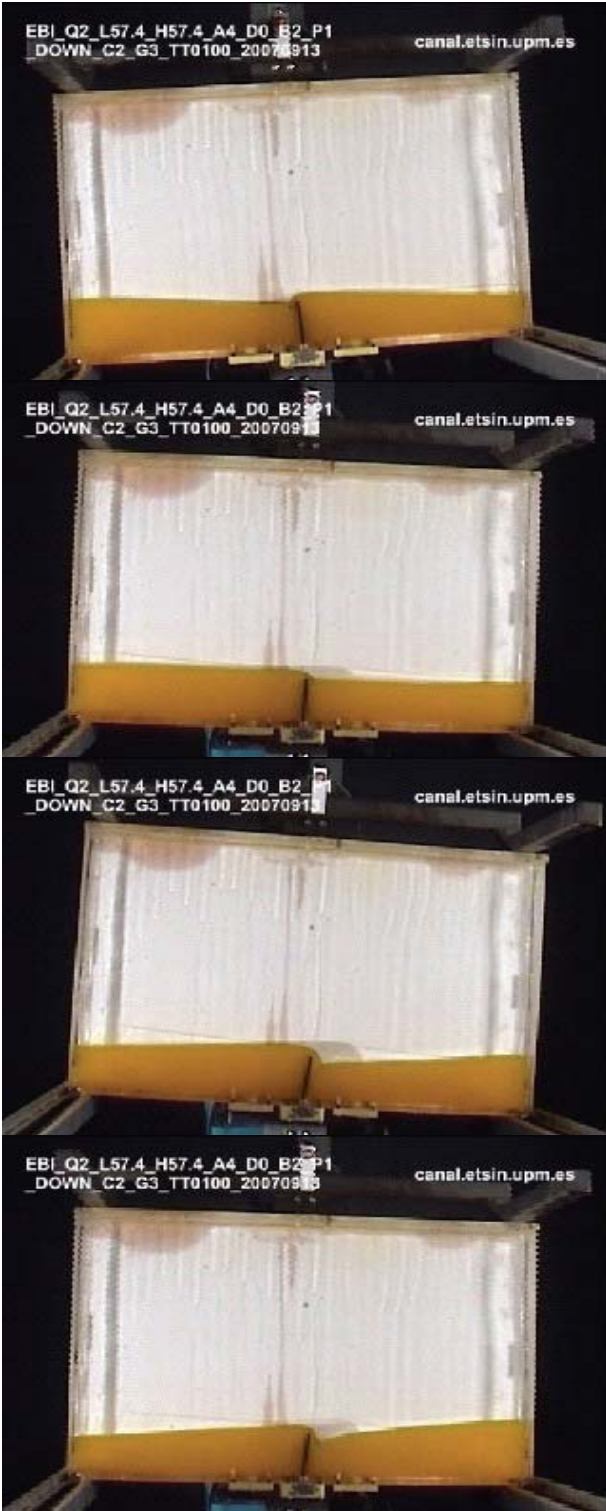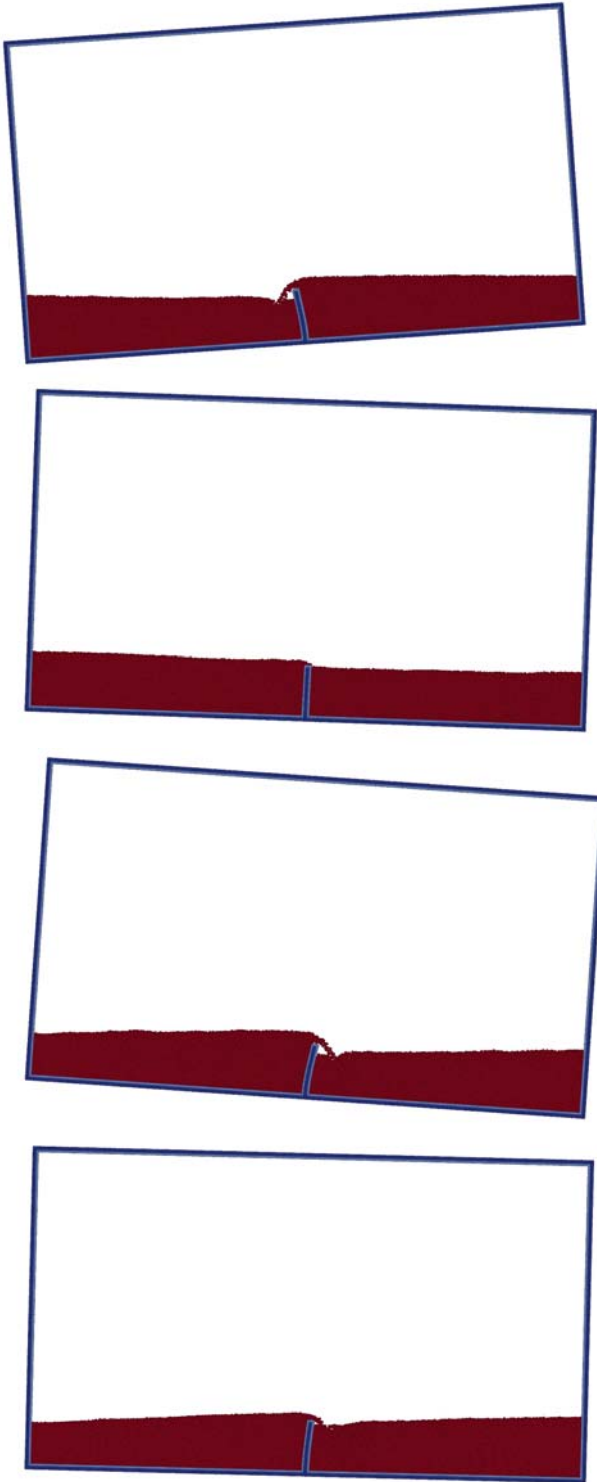
<div align="center">Experiment (Idelsohn, 2008)   Present</div>

Figure 8. Deformation of baffle and elevation of free surface for Case 1: t=0.95, 1.35, 1.62, and 1.88 s.
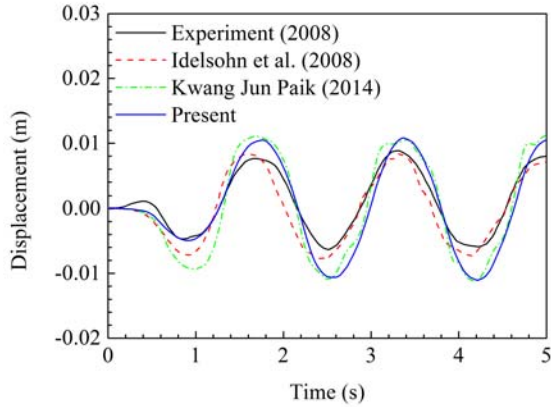
Figure 9. Comparison of the horizontal displacement at the tip of baffle (Case 1)
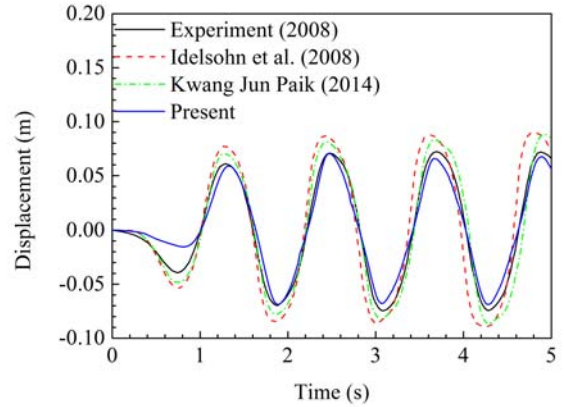
Figure 10. Comparison of the horizontal displacement at the tip of baffle (Case 2)

Elastic beam interacting with deep water flow

In present case, most parameters of simulation are same as that of Case 1. The tank rotates with an amplitude same as that of case 1 but a higher frequency of 0.83 Hz. Level of fluid filled in the tank is twice the depth of case 1. A longer baffle with the length of 114.8 mm is also mounted at the rolling center. The baffle is dispersed by 58 beam elements. The coefficients of $\alpha_1 = 0.0$ and $\alpha_2 = 0.025$ are used in this case. Detailed parameters of the simulation are shown in table 1 and table 2.

Fig. 10 shows the comparison of time histories of the horizontal displacement at the top tip of baffle. Forms of the curves are similar to those in previous case but with larger amplitudes due to a much deeper fluid filled in the tank. According to the figure, both amplitude and period are in good agreement with experimental data.

Snapshots about deformation of the baffle and elevation of free surface are shown in Fig. 11. Numerical data is compared with experiment at eight instants, t=1.69, 1.96, 2.09, 2.23, 2.36, 2.56, 2.69, 2.83 s. The baffle deforms obviously and keep submerged after the instant t=1.69 s. Though the interaction between fluid and the elastic baffle is very strong, both numerical shapes of baffle and free surface are in good agreement with experiment.
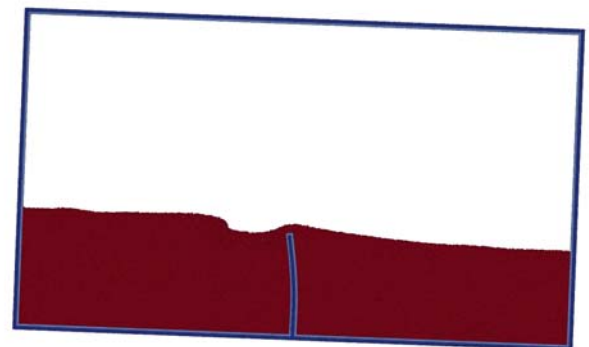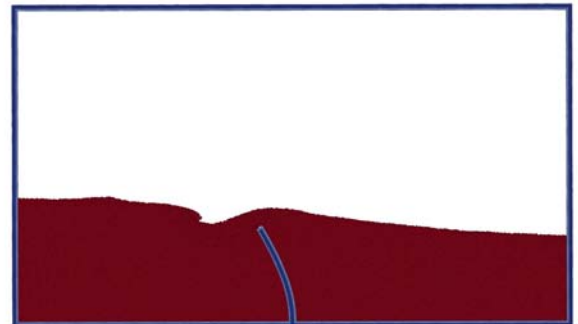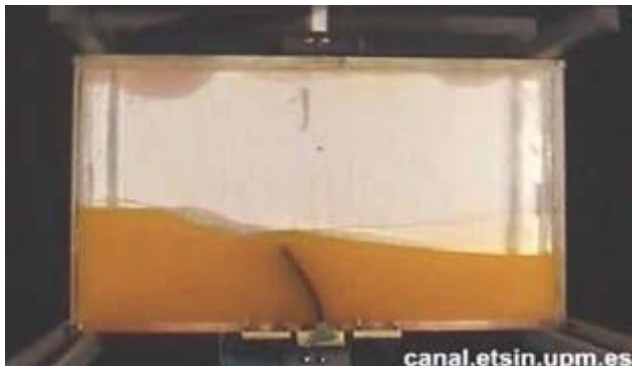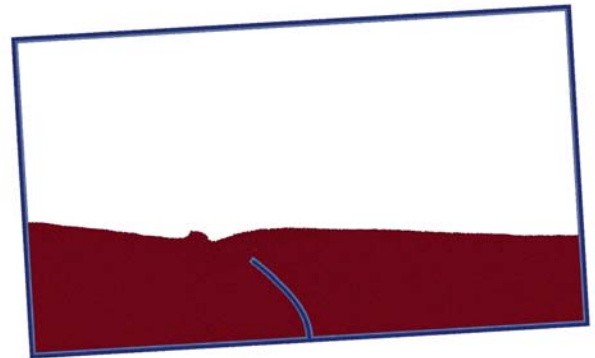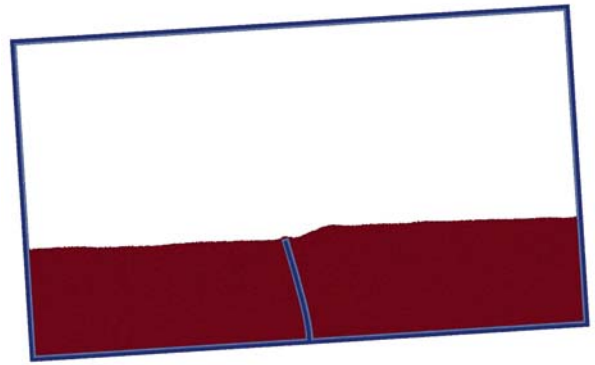
Experiment (Idelsohn, 2008)   Present

Figure 11. **Deformation of baffle and elevation of free surface for Case 2: t=1.69, 1.96, 2.09, 2.23, 2.36, 2.56, 2.69, 2.83 seconds**
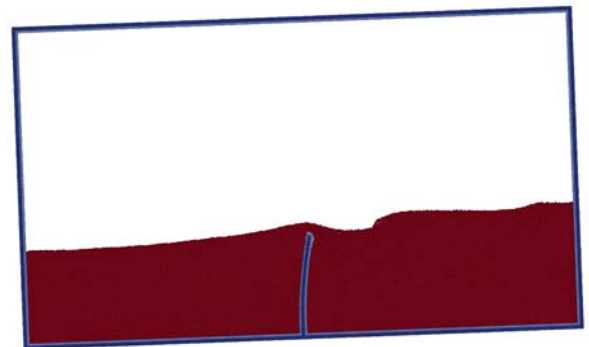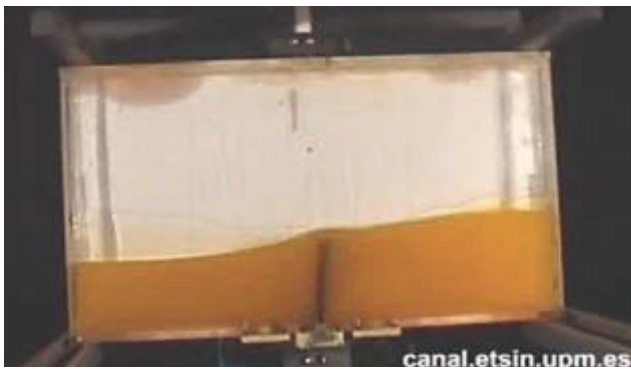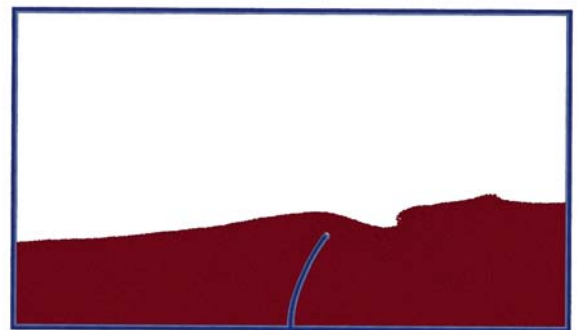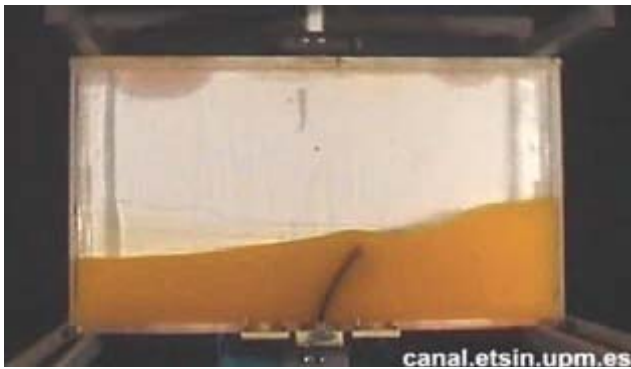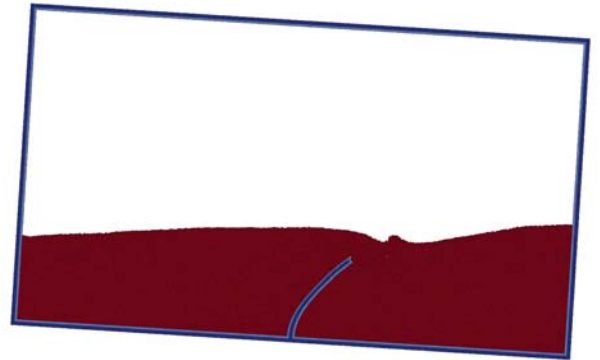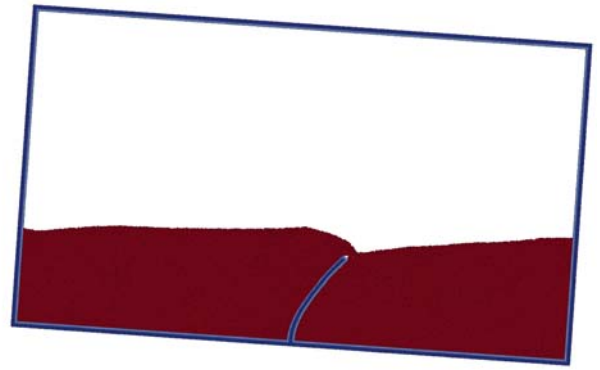
Experiment (Idelsohn, 2008)   Present

Figure 11. Continued

Hanging elastic beam interacting with shallow water flow

This case is much different from Cases 1 and 2. Unlike the arrangements of baffles in previous two cases, the longest baffle is hanging at the top of tank and the end tip reaches to the surface of fluid. So, the deformation of baffle is only caused by the impact force of free surface waves. In this case, the tank is forced to roll with the amplitude of 2 degrees and the frequency of 0.61 Hz. Level of fluid is same as that in case 1. Density and Kinematic viscosity are 998 kg/m^3 and 1×10^{-6} m^2/s, respectively. The baffle is dispersed by 145 beam elements. Density and the Young's modulus of the baffle are 1900 kg/m^3 and 4×10^6 Pa, respectively. The coefficients of $\alpha_1 = 0.0$ and $\alpha_2 = 0.025$ are used in this case. Detailed parameters of the simulation are shown in table 1 and table 2.

Fig. 12 shows the comparison of time histories of the horizontal displacement at the middle and end tip of baffle. According to both experimental and numerical data, deformation of the baffle is highly nonlinear. High frequency oscillation is observed after t=2 s for both middle and tip of the baffle. Though it's much more challenging to obtain the accurate solution, the agreement between present result and experiment is acceptable.

Snapshots about deformation of baffle and elevation of free surface are shown in Fig. 13. Numerical data is compared with experiment at nine instants, t=1.95, 2.42, 2.69, 2.82, 3.02, 3.29, 3.69, 3.89, 4.09 s. Both numerical shapes of baffle and free surface are quite similar to experiment results during the whole process of wave propagation. However, spray around the tip of baffle, caused by the impact between baffle and wave crest, exists at the instances 3.02 and 3.89 s. This phenomenon is not obviously observed from the experimental figures. Possible reasons for the discrepancy between present results and the experiment could be the three dimensional characters. Besides, the effect of rough boundary of the elastic baffle in experiment shouldn't be neglected.
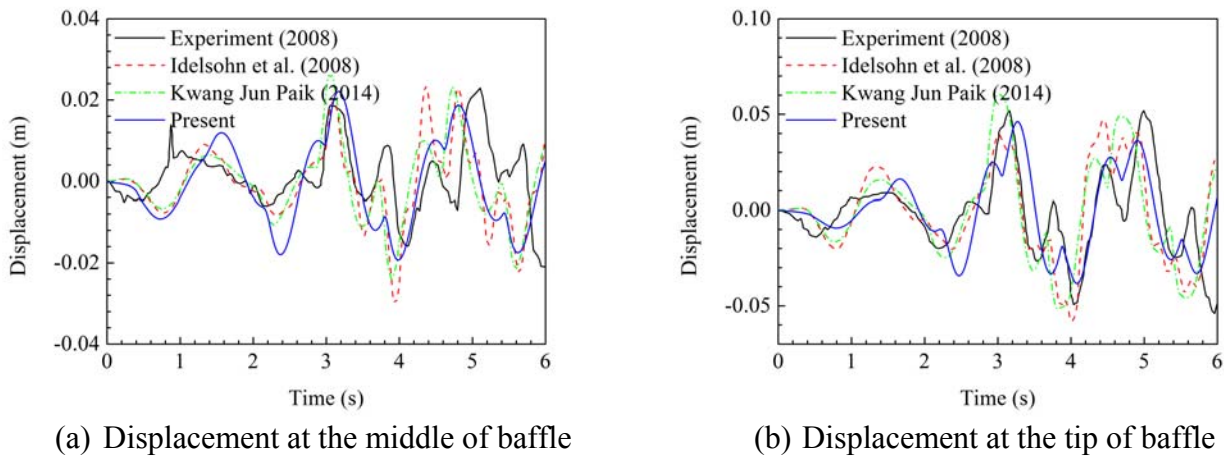
(a) Displacement at the middle of baffle   (b) Displacement at the tip of baffle
Figure 12.   Comparison of the horizontal displacement (Case 3)
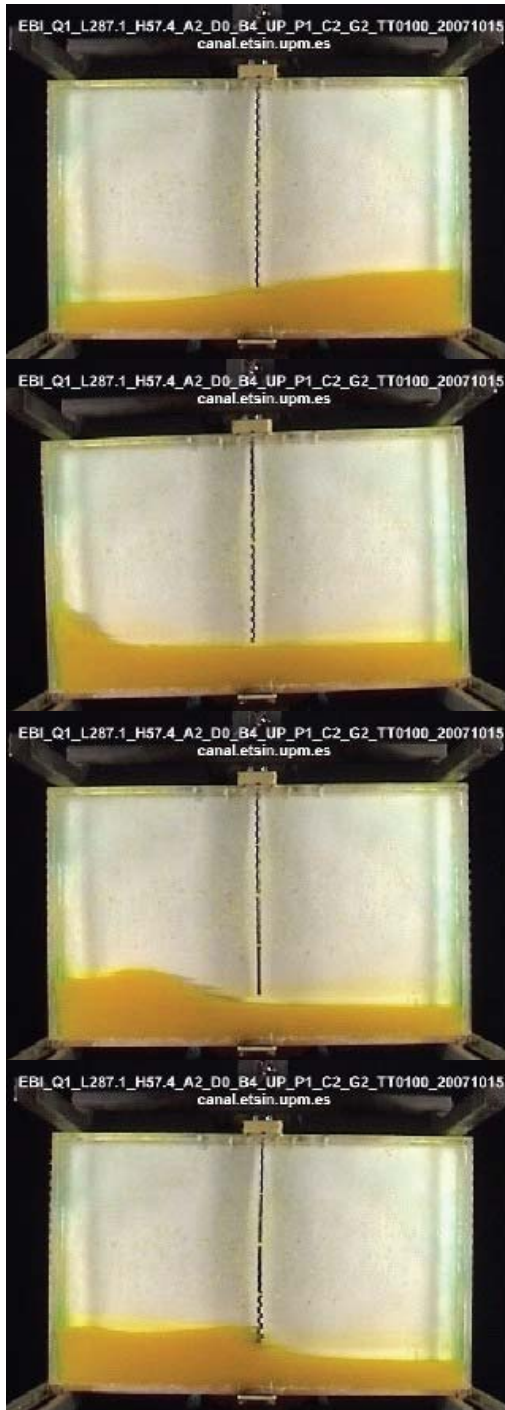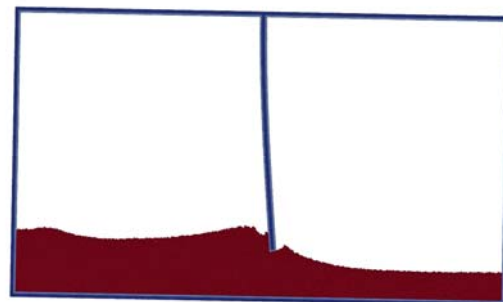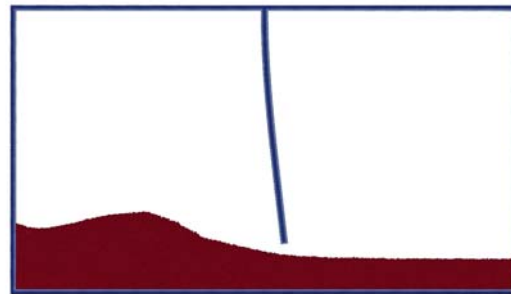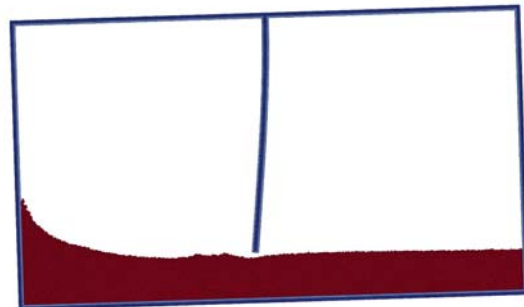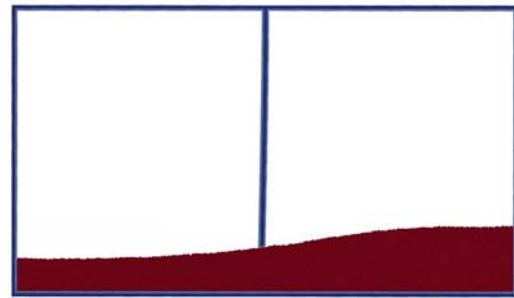
Experiment (Idelsohn, 2008)   Present

**Figure 13.   pressure contours (middle) and velocity vectors (right) for Case 3: t=1.95,
2.42, 2.69, 2.82, 3.02, 3.29, 3.69, 3.89, 4.09 seconds (Continued)**
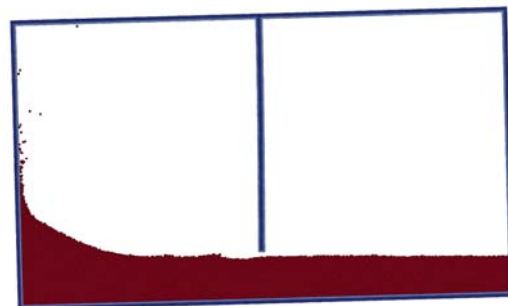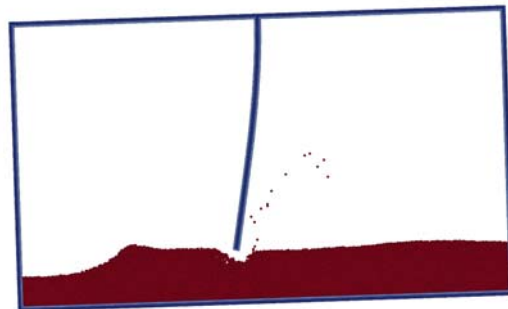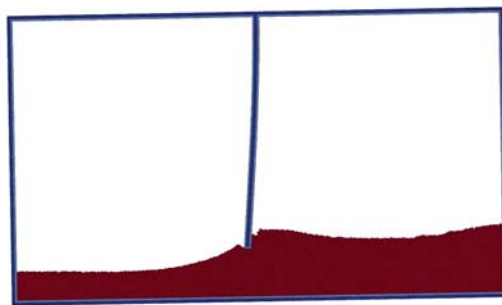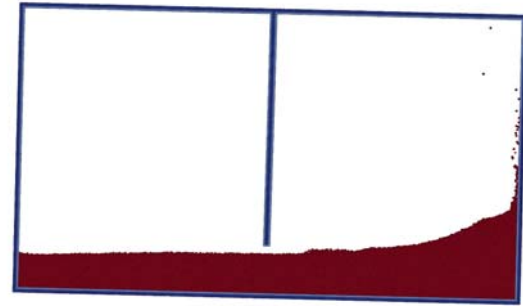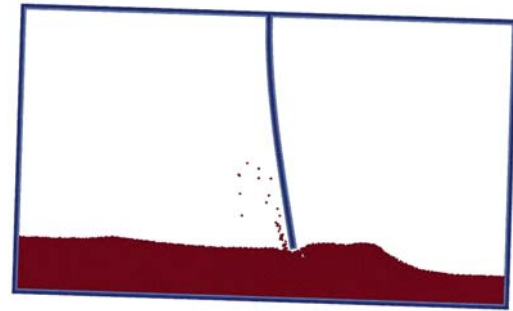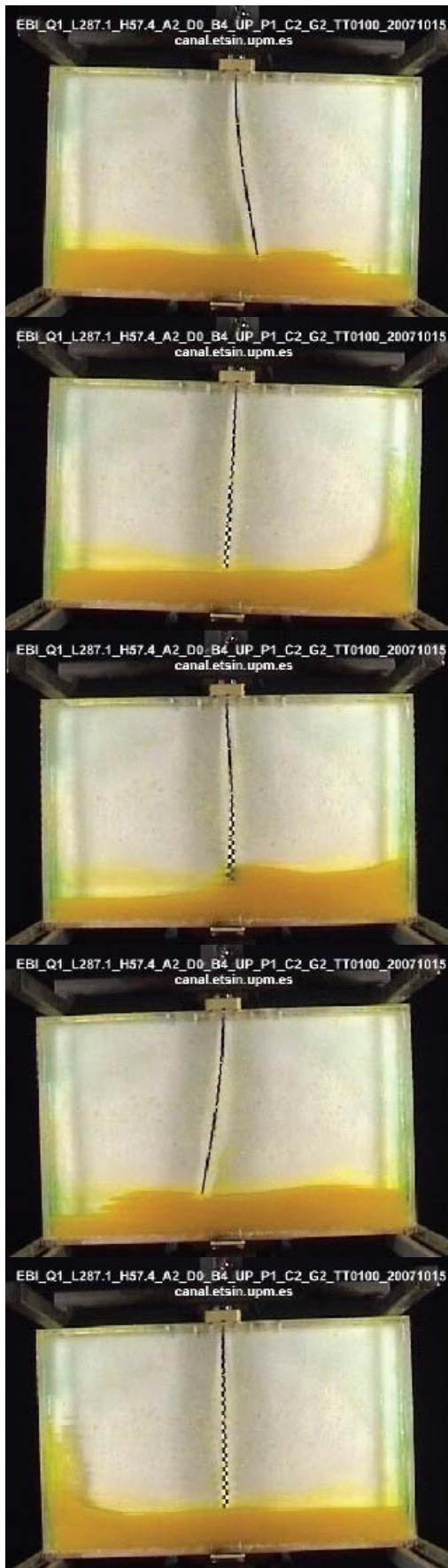
Figure 13. Continued

Conclusions

The aim of this paper is to develop a MPS-FEM coupled method for fluid structure interaction problems and validate the capability of this method. Mathematical equations for the MPS and FEM method, together with the coupling strategy, are described firstly. According to two dynamic tests, the proposed structural solver is accurate enough for structural deformation problems. Then, the FSI problems of sloshing with elastic baffles are numerically studied by the MPS-FEM coupled method. Deformations of the baffles, include the linear and nonlinear responses, are quite coincident between present numerical results and experiment. Present numerical results show that the proposed MPS-FEM coupled method is capable of simulating problems about structural deformation interaction with violent free surface flow.

References

[1] Zhang, Y. X., Wan, D. C., Hino, T. (2014) Comparative study of MPS method and level-set method for sloshing flows, *Journal of hydrodynamics* **26**(4), 577-585.

[2] Zhang, Y. L., Tang, Z. Y., and Wan, D. C. (2016) Numerical Investigations of Waves Interacting with Free Rolling Body by Modified MPS Method, *International Journal of Computational Methods* **13**(4), 1641013.

[3] Koshizuka, S., and Oka, Y. (1996) Moving particle Semi-implicit Method for Fragmentation of Incompressible Fluid, *Nuclear Science and Engineering* **123**, 421-434.

[4] Khayyer, A., and Gotoh, H. (2009) Modified Moving Particle Semi-implicit methods for the prediction of 2D wave impact pressure, *Coastal Engineering* **56**, 419-440.

[5] Khayyer, A., and Gotoh, H. (2010) A higher order Laplacian model for enhancement and stabilization of pressure calculation by the MPS method, *Applied Ocean Research* **32**, 124-131.

[6] Khayyer, A., and Gotoh, H. (2011) Enhancement of stability and accuracy of the moving particle semi-implicit method, *Journal of Computational Physics* **230**, 3093-3118.

[7] Khayyer, A., and Gotoh, H. (2012) A 3D higher order Laplacian model for enhancement and stabilization of pressure calculation in 3D MPS-based simulations, *Applied Ocean Research* **37**, 120-126.

[8] Kondo, M., and Koshizuka, S. (2011) Improvement of stability in moving particle semi-implicit method, *Int. J. Numer. Meth. Fluids* **65**, 638-654.

[9] Tanaka, M., and Masunaga, T. (2010) Stabilization and smoothing of pressure in MPS method by Quasi-Compressibility, *Journal of Computational Physics* **229**, 4279-4290.

[10] Ikari, H., Khayyer, A., and Gotoh. H. (2015) Corrected higher order Laplacian for enhancement of pressure calculation by projection-based particle methods with applications in ocean engineering, *J. Ocean Eng. Mar. Energy* **1**(4), 361-376.

[11] Zhang, Y. X., and Wan, D. C. (2011) Application of MPS in 3D Dam Breaking Flows, *Sci. Sin. Phys. Mech. Astron.* **41**, 140-154.

[12] Lee, B. H., Park, J. C., Kim, M. H., Jung, S. J., Ryu, M. C., and Kim, Y. S. (2010). Numerical simulation of impact loads using a particle method, *Ocean Engineering* **37**, 164-173.

[13] Yokoyama, M., Kubota, Y., Kikuchi, K., Yagawa, G., and Mochizuki, O. (2014). Some remarks on surface conditions of solid body plunging into water with particle method, *Advanced Modeling and Simulation in Engineering Sciences* **1**(1), 1-14.

[14] Hwang, S. H., Khayyer, A., Gotoh, H., and Park, J. C. (2015). *Simulations of Incompressible Fluid Flow-Elastic Structure Interactions by a Coupled Fully Lagrangian Solver*, Proc 25th Int Offshore and Polar Eng Conf, Hawaii, ISOPE, 1247-1250.

[15] Koshizuka, S., Shibata, K., Tanaka, M. and Suzuki, Y. (2007) *Numerical analysis of fluid-structure and fluid-rigid body interactions using a particle method*, Proceedings of FEDSM2007, San Diego, California USA.

[16] Sueyoshi, M., Kashiwagi, M., and Naito, S. (2008) Numerical simulation of wave-induced nonlinear motions of a two-dimensional floating body by the moving particle semi-implicit method, *J. Mar. Sci. Technol* **13**, 85-94.

[17] Zhang, Y. X., and Wan, D. C. (2012) *Apply MPS Method to Simulate Liquid Sloshing in LNG Tank*, Proc. 22nd Int. Offshore and Polar Eng. Conf., Rhodes, Greece, 381-391.

[18] Tang, Z. Y., and Wan, D.C. (2015) Numerical simulation of impinging jet flows by modified MPS method, *Engineering Computations* **32**(4), 1153-1171.

[19] Sun, Z., Xing, J. T., Djidjeli, K. and Cheng, F. (2015) *Coupling MPS and Modal Superposition Method for Flexible Wedge Dropping Simulation*, Proceedings of the Twenty-fifth International Ocean and Polar Engineering Conference, Kona, Big Island, Hawaii, USA, 144-151.

[20] Onate, E., Idelsohn, S. R., Celigueta, M. A., Rossi, R. (2006) *Advances in the particle finite element method for fluid-structure interaction problems*, In: Proceedings of 1st South-East European Conference on Computational Mechanics, SEECCM-06, Kragujevac, Serbia and Montenegro.

[21] Idelsohn, S. R., Marti, J., Limache, A. and Onate, E. (2008) Unified Lagrangian formulation for elastic solids and incompressible fluids: Application to fluid-structure interaction problems via the PFEM, *Comput. Methods Appl. Mech. Eng* **197**, 1762-1776.

[22] Ryzhakov, P. B., Rossi, R., Idelsohn, S. R. and Onate, E. (2010) A monolithic Lagrangian approach for fluid-structure interaction problems, *Comput. Mech* **46**, 883-899.

[23] Liao, K. P., Hu, C. H. (2013) A coupled FDM-FEM method for free surface flow interaction with thin elastic plate, *J. Mar. Sci. Technol* **18**, 1-11.

[24] Mitsume, N., Yoshimura, S., Murotani, K., Yamada, T. (2014a) MPS-FEM partitioned coupling approach for fluid-structure interaction with free surface flow, *International Journal of Computational Methods* **11**(4), 4157-4160.

[25] Mitsume, N., Yoshimura, S., Murotani, K., Yamada, T. (2014b) Improved MPS-FE Fluid-Structure Interaction Coupled Method with MPS Polygon Wall Boundary Model, *Comput. Model. Eng. Sci* **101**(4), 229-247.

[26] Hou, G., Wang, J., Layton, A. (2012) Numerical Methods for Fluid-Structure Interaction - A Review, *Commun. Comput. Phys* **12**(2), 337-377.

[27] Longatte, E., Verremana, V., Souli, M. (2009) Time marching for simulation of fluid-structure interaction problems, *Journal of Fluids and Structures* **25**, 95-111.

[28] Heil, M., Hazel, A. L., Boyle, J. (2008) Solvers for large-displacement fluid-structure interaction problems: segregated versus monolithic approaches, *Computational Mechanics* **43**(1), 91-101.

[29] Iura, M., Atluri, S. N. (1995) Dynamic analysis of planar flexible beams with finite rotations by using inertial and rotating frames, *Computers and Structures* **55**(3), 453-462.

[30] Newmark, N. M. (1959) A method of computation for structural dynamics, *Journal of the engineering mechanics division* **85**(3), 67-94.

[31] Hsiao, K. M., Lin, J. Y., Lin, W. Y. (1999) A consistent co-rotational finite element formulation for geometrically nonlinear dynamic analysis of 3-D beams, *Comput. Methods Appl. Mech. Engrg* **169**, 1-18.

[32] Paik, K. J. (2010) Simulation of fluid-structure interaction for surface ships with linear/nonlinear deformations, University of Iowa, thesis for PhD degree.

[33] Paik, K. J., and Carrica, P. M. (2014) Fluid-structure interaction for an elastic structure interacting with free surface in a rolling tank, *Ocean Engineering* **84**, 201-212.

[34] Behdinan, K., Stylianou, M. C., Tabarrok, B. (1998) Co-rotational dynamic analysis of flexible beams, *Comput. Methods Appl. Mech. Eng* **154**, 151-161.